Metal–Organic Frameworks

International Edition: DOI: 10.1002/anie.201802661
German Edition: DOI: 10.1002/ange.201802661

Pore-Environment Engineering with Multiple Metal Sites in Rare-Earth Porphyrinic Metal–Organic Frameworks

Liangliang Zhang[+], Shuai Yuan[+], Liang Feng[+], Bingbing Guo, Jun-Sheng Qin, Ben Xu, Christina Lollar, Daofeng Sun, and Hong-Cai Zhou**

Abstract: *Multi-component metal–organic frameworks (MOFs) with precisely controlled pore environments are highly desired owing to their potential applications in gas adsorption, separation, cooperative catalysis, and biomimetics. A series of multi-component MOFs, namely PCN-900(RE), were constructed from a combination of tetratopic porphyrinic linkers, linear linkers, and rare-earth hexanuclear clusters (RE_6) under the guidance of thermodynamics. These MOFs exhibit high surface areas (up to 2523 $cm^2 g^{-1}$) and unlimited tunability by modification of metal nodes and/or linker components. Post-synthetic exchange of linear linkers and metalation of two organic linkers were realized, allowing the incorporation of a wide range of functional moieties. Two different metal sites were sequentially placed on the linear linker and the tetratopic porphyrinic linker, respectively, giving rise to an ideal platform for heterogeneous catalysis.*

Multi-component metal–organic frameworks (MOFs) with synergistic functionalities in a designed cavity are particularly interesting because of their potential applications in gas adsorption, separation, cooperative catalysis, and biomimetics.[1] Pioneering work has been demonstrated by Yaghi and co-workers by incorporating up to eight functional groups into multivariate MOFs (MTV-MOFs), which showed emergent properties distinct from their parent frameworks.[2] However, this method typically lacks a high level of control over the positions of functional groups, as functional groups tend to be disordered in the crystal lattice. To address this issue, Telfer and co-workers demonstrated a strategy to incorporate different functional groups on linkers of various connectivity and symmetry in pre-determined positions of a mixed-linker MOF.[3] Still, this strategy only works for a limited number of MOFs, which require linkers with exactly matched sizes and symmetries. Later on, our group introduced a post-synthetic method, linker installation, to engineer pore environments with precisely placed linkers in zirconium MOFs.[4] However, it is still challenging to incorporate multiple metal sites in pre-determined positions within a MOF cavity.[5]

To this end, rare-earth (RE)-metal-based clusters seem to be suitable building units for the development of MOFs with multiple metal sites. Owing to the chemical similarity of RE elements, different RE metals tend to form similar SBUs and isostructural MOFs, providing additional tunability by tuning the metals in RE-MOFs. Furthermore, the rare-earth metals can form 12-connected hexanuclear $RE_6(OH)_8(COO)_{12}$ clusters,[6] similar to the well-studied $Zr_6O_4(OH)_4(COO)_{12}$ in many Zr-MOFs.[7] Therefore, it is expected that the knowledge in the design of mixed-linker Zr-MOFs can be applied to RE-MOF systems. Compared with Zr-MOFs, RE-MOFs are usually fluorescent owing to f–f transitions, which offers potential applications in the manufacture of electroluminescent devices, fluorescent probes, and photocatalysts.[8] Further incorporation of multiple functionalities inside RE-MOFs might generate structures with interesting properties and applications. Bearing this in mind, we assembled a series of multi-component RE-MOFs, namely PCN-900(RE), using a combination of tetratopic porphyrinic linkers, linear linkers, and $RE_6(OH)_8(COO)_{12}$ clusters. Pore environment engineering with multiple metal sites was realized in these MOFs, which led to the formation of mesopores decorated by high-density metal sites. Furthermore, PCN-900(RE) is an ideal platform for heterogeneous catalysis. As a proof-of-concept, we explored their catalytic performances in the cycloaddition of CO_2 and epoxides.

A thermodynamically guided strategy was utilized to synthesize mixed-component RE-MOFs. This strategy has been effective for the design and synthesis of mixed-linker Zr-MOFs with Zr_6, a structural analogue to RE_6 clusters.[6] In this strategy, a primary linker is selected which will form MOFs with coordinatively unsaturated Zr_6 or RE_6 clusters as thermodynamically unstable intermediates. An auxiliary linker will be subsequently added to the system, which will insert into these coordinatively unsaturated clusters to fulfill the 12-connectivity of the metal nodes. A tetratopic porphyrinic linker, TCPP was adopted as a primary linker because it shows great potential towards applications including sensing, bio-mimetic catalysis, and solar cells [TCPP = tetrakis(4-carboxyphenyl)porphyrin)]. Intuitively, the combination of 4-connected TCPP and 12-connected RE_6 clusters can generate a RE-MOF with a (4, 12)-connected ***ftw*** network isostructural to MOF-525.[9] However, the ***ftw*** network requires four phenyl rings to be coplanar with the porphyrin

[*] L.-L. Zhang,[+] B.-B. Guo, B. Xu, Prof. Dr. D.-F. Sun
College of Science, China University of Petroleum (East China)
Qingdao, Shandong 266580 (China)
E-mail: dfsun@upc.edu.cn
S. Yuan,[+] L. Feng,[+] J.-S. Qin, C. Lollar, Prof. Dr. H.-C. Zhou
Department of Chemistry
Texas A&M University, College Station, TX 77843 (USA)
E-mail: zhou@chem.tamu.edu
Prof. Dr. H.-C. Zhou
Department of Materials Science and Engineering
Texas A&M University, College Station, TX 77842 (USA)
[+] These authors contributed equally to this work.
Supporting information and the ORCID identification number(s) for the author(s) of this article can be found under: https://doi.org/10.1002/anie.201802661.

in TCPP, representing an unfavorable conformation and a thermodynamically unstable product. Alternatively, the connectivity of RE_6 clusters can be reduced to 6 or 8-connected to form PCN-224[10] or PCN-222[11] isostructures. However, partially eliminating the coordinated carboxylates on a RE_6 cluster will inevitably destabilize the framework. Therefore, the synthesis of MOFs based on RE_6 and TCPP was unsuccessful. The RE_6 cluster tends to undergo a rearrangement to form RE-oxo chains as thermodynamically favored products. We propose that the RE-MOF isostructural to PCN-224 can be obtained by using an auxiliary linker DCDPS (DCDPS = 4,4′-dicarboxydiphenyl sulfone), which bridges the coordinatively unsaturated RE to fulfill the 12-connected nodes. From a thermodynamics perspective, the DCDPS, with its suitable size and geometry, will occupy the uncoordinated sites of the RE_6 cluster, forming a fully connected $RE_6(OH)_8(COO)_{12}$ cluster based RE-MOF as the thermodynamic product (Scheme 1). As expected, solvothermal reactions of TCPP, DCDPS, and $Eu(NO_3)_3{\cdot}6H_2O$ in the presence of 2-fluorobenzoic acid (2-FBA) in N,N′-dimethylformamide (DMF) at 120 °C yielded cubic crystals of PCN-900(Eu).

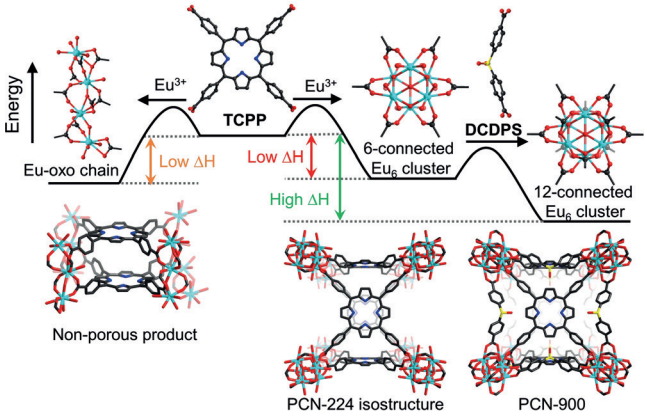

Scheme 1. Thermodynamically guided synthesis of multivariate porphyrinic RE-MOFs.

To study the effect of auxiliary linker DCDPS on the formation of PCN-900(Eu), the synthesis was carried out under different linker ratios. Since PCN-900(Eu) exhibits cubic crystals, the phase purity could be directly observed from optical images. The identity of products was further confirmed by powder X-ray diffraction (PXRD). Without the adjunction of DCDPS, only some low-crystalline products formed which is attributed to the non-porous RE-TCPP MOF composed of RE-oxo chains. With an increased DCDPS ratio, PCN-900(Eu) starts to form, while low-crystalline products still exist as impurity. When the molar ratio between DCDPS and TCPP reaches 25:1, pure PCN-900(Eu) phase is obtained (Figure 1). These results highlight the important role of DCDPS to induce the formation of thermodynamically stable PCN-900(Eu).

Single-crystal X-ray diffraction studies have revealed that PCN-900(Eu) crystallized in space group $Im\bar{3}m$ and was formulated as $[(CH_3)_2NH_2]_2[Eu_6(\mu_3\text{-}OH)_8(TCPP)_{1.5}\text{-}(DCDPS)_3]\cdot(solvent)_x$. This framework consists of Eu_6 clusters linked by bent, ditopic DCDPS linkers and square-planar TCPP linkers. Each Eu_6 cluster was connected by six TCPP linkers to form the scaffold structure which is isostructural to PCN-224.[10] The scaffold structure can be simplified into a 4,6-connected net with ***she*** topology (Figure 2a). The DCDPS linker bridges a pair of neighboring Eu_6 cluster to fulfill the 12 connectivity. Topologically, the 12-connected metal clusters and tetratopic TCPP linkers can be regarded as cuboctahedron and square nodes, respectively. The overall structure was analyzed to be a 4,12-connected net with a point symbol of $\{3^{12}.4^{18}.5^{24}.6^{12}\}_2\{3^4.4^2\}_3$, determined by TOPOS 4.0 (Figure 2b). This topology was named as ***tam*** and included in the reticular chemistry structure resource (RCSR) database. The free volume of PCN-900(Eu) is up to 78.6% based on the calculation by PLATON software.

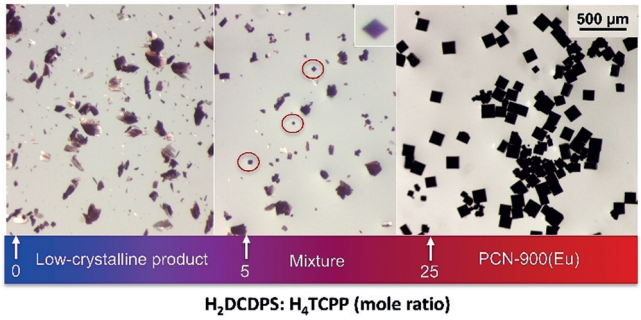

Figure 1. Different phases are yielded depending on the ratio of the components in solution. An optimal mole ratio of H_2DCDPS and H_4TCPP to produce PCN-900(Eu) is larger than 25:1. Arrows below each picture indicate the mole ratio used to generate the product shown.

The metal components in PCN-900(RE) are highly tunable. PCN-900(RE) analogues with various RE metals (that is, Eu, Y, Yb, Tb, Dy) have also been successfully synthesized under similar reaction conditions (Figure 2c). Furthermore, the porphyrin center of PCN-900(Eu) can be metalated by first-row transition metals simply through incubating the single-crystals of PCN-900(Eu) in a solution of MCl_2 (M = Zn, Fe, Co, Ni). The resultant MOFs, namely PCN-900(Eu)-MTCPP, well maintain their crystallinity and the incorporated metal ions into the porphyrin center can be clearly observed in the single structures (Figure 2d). Element mapping performed by SEM-EDS indicates a uniform distribution of metals and TCPP linkers throughout the crystal, suggesting a homogeneous crystalline framework (Supporting Information, Figure S1). XPS of PCN-900(Eu) series further indicates the existence of post-synthetically incorporated metal species (Supporting Information, Figures S3–S6). Note that PCN-900(Eu)-MTCPP can also be synthesized in a one-pot reaction using metalloporphyrin linkers as starting materials.

Interestingly, the Eu-DCDPS bond is distorted in PCN-900(Eu). Normally, the carboxylates from linkers should be coplanar to the adjacent O-Eu-Eu-O plane. However, the Eu-DCDPS junction is severely twisted in PCN-900(Eu) with the carboxylate bent 49 degree away from its normal position

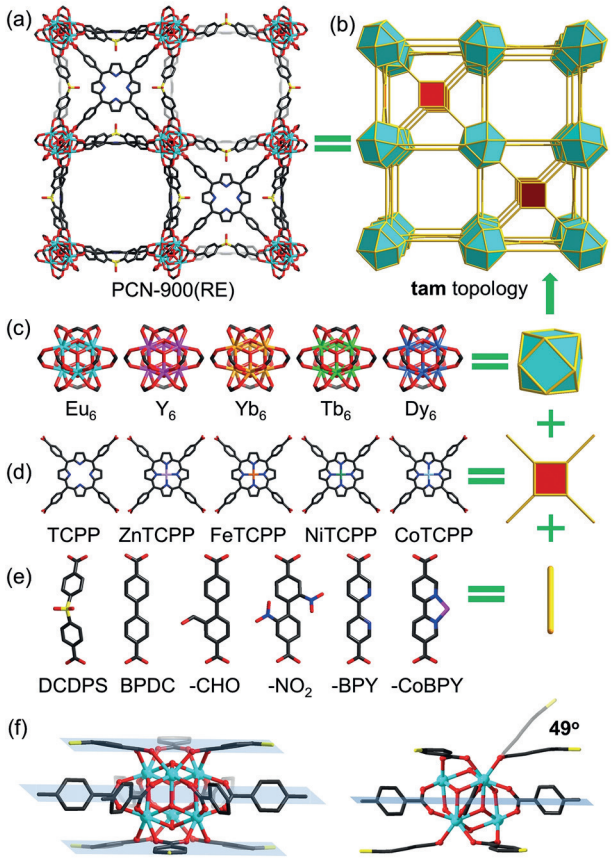

Figure 2. a) Crystal structure and b) underlying ***tam*** topology of PCN-900 (Eu); c) 12-connected RE_6 cluster (RE = Eu, Y, Yb, Tb and Dy); d) MTCPP used in this work (M = no metal, Zn, Fe, Ni, and Co); e) linear linkers with different functionalities used in this work; f) twisted dihedral angle between the O-Eu-Eu-O plane and the DCDPS carboxylate. Eu green, C black, O red, N blue, H white.

(Figure 2 f). The Eu-carboxylate junction between the Eu_6 cluster and the TCPP linker shows a normal conformation. We propose that the unusual bond angle may destabilize the binding between the DCDPS and the framework and it can be changed by other linear linkers with suitable lengths.

As expected, the bent DCDPS linker can be replaced by linear linkers such as BPDC and its derivatives to form a series of functionalized MOFs. Functional groups, including −CHO, $-NO_2$, and −bipyridyl were incorporated inside PCN-900(Eu) by exchanging the auxiliary linker (Figure 2 e). The ratio of exchanged linker was further confirmed by ^{1}H NMR (Supporting Information, Figures S7–S11). Single crystals of both partially and fully exchanged PCN-900(Eu) were obtained. The intermediate state of partially exchanged PCN-900(Eu) unambiguously supports the exchange process, rather than a dissolution–recrystallization process. Additionally, the supernatant was further separated and analyzed by UV and ICP, showing only negligible TCPP or Eu releasing during the exchange. TEM and SEM images (Supporting Information, Figures S1, S2) indicates the maintained morphology of MOF particles after linker exchange. PXRD of exchanged sample also shows a well-maintained crystallinity in the bulk material. These results indicate the successful linker exchange of PCN-900(Eu). Direct synthesis of PCN-900(Eu) using BPDC as auxiliary linker was unsuccessful because BPDC tend to form ***fcu*** networks with stable 12-connnected Eu_6 clusters which compete with the formation of PCN-900(Eu). The crystal data and structure refinements of PCN-900 series are summarized in the Supporting Information, Table S1.

The permanent porosity of the PCN-900 series is confirmed by N_2 adsorption isotherms measured at 77 K (Figure 3, S12-23). Prior to the gas sorption measurements, PCN-900 series samples were rinsed thoroughly using DMF

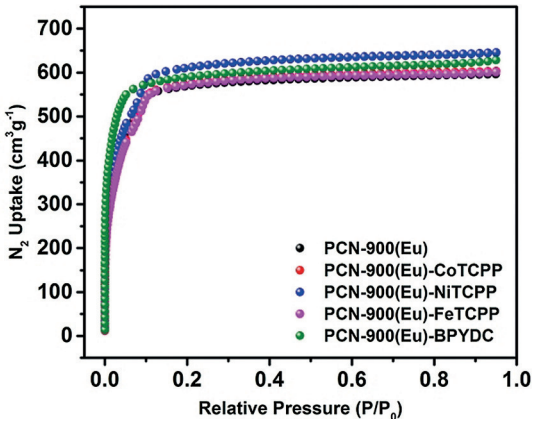

Figure 3. N_2 adsorption isotherms of PCN-900(Eu) and its derivatives at 77 K, 1 atm. Desorption branches of isotherms are omited for clarity.

and fresh acetone for three days before thermal activation at 100 °C under vacuum. PCN-900(Eu)-NiTCPP exhibits a saturated uptake of 645 $cm^3 g^{-1}$ at 1 atm and Brunauer–Emmett–Teller (BET) surface area of 2523 $m^2 g^{-1}$. The calculated total pore volume of PCN-900(Eu)-NiTCPP is 1.01 $cm^3 g^{-1}$. Other PCN-900(Eu) series with different metalloporphyrins or functionalized linkers also show similar N_2 adsorption isotherms and surface areas. These results indicate the successful functionalization of PCN-900(Eu) using different metals or functional groups while maintaining the porous structure. The stability of PCN-900(RE) was examined by soaking MOFs in various solvents for 24 h. PXRD patterns suggest that PCN-900(RE) has remarkable stability since it retains crystallinity in most solvents including DMF, acetone, CH_3OH, EtOH, CH_3CN, and water (Supporting Information, Figure S24, S25), which is significant to many applications. Thus, PCN-900(RE) series show excellent thermal stability according to the results of thermogravimetric analyses (Supporting Information, Figures S26–28).

PCN-900(Eu)-TCPP-BPYDC is an ideal platform for pore environment engineering due to the fact that multiple metal sites arrange at predetermined positions within a MOF cavity. We demonstrated that metal sites can be arranged at the vertexes (RE_6 clusters), edges (MBPYDC), and faces (MTCPP) of a cubic cage. With large pores decorated with highly accessible metal sites, PCN-900(Eu)-CoTCPP-CoBPYDC represents a suitable platform to incorporate metal

catalysts. As a proof of concept, PCN-900(Eu)-CoTCPP-CoBPYDC was assembled by the metalation of PCN-900-(Eu)-TCPP-BPYDC with Co^{2+}. To illustrate the free accessibility of the multiple metal sites, we explored their catalytic performances in the cycloaddition of CO_2 and epoxides.[12]

Cycloaddition of CO_2 with epoxides is a green process and atom economy reaction to convert CO_2 into valuable chemicals, including urea, cyclic carbonates, and formic acid. It requires high surface area, enough Lewis acidic sites, and high chemical stability to afford efficient heterogeneous catalysts. We choose the cycloaddition of CO_2 with epoxides as a representative reaction to evaluate the Lewis acid catalytic activity of PCN-900 series. The performances of different MOF catalysts in the cycloaddition of CO_2 and epoxides were compared in Table 1. PCN-900(Eu)-CoTCPP-CoBPYDC,[6g,13] a MOF formed by Eu_6 clusters and CoBPYDC is less active than PCN-900(Eu)-CoTCPP-CoBPYDC because of the limited pore size. Even the physical mixture of two individual functionalities demonstrates much lower conversion than the MTV-PCN-900(Eu), suggesting the integrated whole is better than the sum of individuals. The substrate scope is further explored. As shown in Table 1, different epoxides were converted in high yields. Moreover, PCN-900(Eu)-CoTCPP-CoBPYDC was recycled for subsequent runs under the same conditions. After three catalysis cycles, the catalytic activity and crystallinity were still well-maintained, as indicated by PXRD (Supporting Information, Figure S29). Among all the representative MOF catalysts for CO_2 cycloaddition with epoxides, PCN-900(Eu)-CoTCPP-CoBPYDC shows decent yield under relatively mild conditions (Supporting Information, Table S3). Overall, mesoporous structures with multiple metal sites result in highly efficient catalysis for cycloaddition reactions of CO_2 with epoxides.

Table 1: Cycloaddition reactions of CO_2 with epoxides.[a]

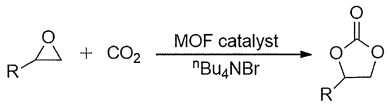

Entry	R	Catalyst	Conversion [%][b]
1	Me	–	15
2	Me	PCN-900(Eu)-BPYDC	32
3	Me	PCN-900(Eu)-CoTCPP	40
4	Me	PCN-900(Eu)-CoTCPP-CoBPYDC	93
5	Me	Eu_6-CoBPYDC	67
6	Me	Eu_9-CoTCPP	44
7	Me	Eu_6-CoBPYDC and Eu_9-CoTCPP	64
8	Et	PCN-900(Eu)-CoTCPP-CoBPYDC	98
9	Ph	PCN-900(Eu)-CoTCPP-CoBPYDC	81
10	CH_2Cl	PCN-900(Eu)-CoTCPP-CoBPYDC	74
11	Me	PCN-900(Eu)-CoTCPP-CoBPYDC, Recycle 1	93
12	Me	PCN-900(Eu)-CoTCPP-CoBPYDC, Recycle 2	91
13	Me	PCN-900(Eu)-CoTCPP-CoBPYDC, Recycle 3	88

[a] Reaction condition: epoxides (5 mmol), MOF catalyst (0.006 mmol based on Co), $^nBu_4NBr$ (0.216 mmol), 50 °C, 20 h, 1 bar CO_2; for Entry 2, 10 mg MOF catalyst was added instead. [b] Conversion was determined by ^1H NMR spectroscopy.

CoBPYDC could function as a highly active heterogeneous catalyst under mild conditions. The Co species play an important role in cycloaddition reactions of CO_2 with epoxides and the amount of cobalt in the corresponding MOFs was calculated from ICP-MS (Supporting Information, Table S2). PCN-900(Eu)-CoTCPP-CoBPYDC presents evidently higher conversion (93%) than its non-metalated (32%) or partial metalated (40%) counterparts. Additionally, the advantage of the PCN-900(Eu) system has also been demonstrated by controlled experiments. Eu_9-CoTCPP,[6c] a MOF based on Eu_9 clusters and CoTCPP, shows much lower yield (44%) compared with that of PCN-900(Eu)-CoTCPP-CoBPYDC. Indeed, Eu_9-CoTCPP has a much smaller pore size (ca. 1.2 nm) than PCN-900(Eu)-CoTCPP-CoBPYDC, which hinders substrate diffusion. Similarly, Eu_6-

In conclusion, a series of multicomponent RE-MOFs were designed and synthesized under the guidance of thermodynamics. The judicious choice of DCDPS as an auxiliary linker permits the formation of PCN-900(RE) with 12-connected RE_6 clusters as the thermodynamically favored product. These MOFs demonstrate high porosity with N_2 total uptakes of 645 $cm^3 g^{-1}$ and BET surface areas up to 2523 $cm^2 g^{-1}$. PCN-900(RE) offers high tunability of both metal and linker components. Post-synthetic exchange DCDPS with linear linkers and metalation of both bipyridyl linkers and porphyrinic linkers were realized to incorporate different metal sites at pre-determined position inside a RE-MOF. The high accessibility of these metal sites was proven by the catalytic cycloaddition reactions of CO_2 with epoxides. We believe that PCN-900(RE) would be especially useful if different metal sites at specific positions are required.

Acknowledgements

The gas adsorption–desorption studies of this research was supported by the Center for Gas Separations Relevant to Clean Energy Technologies, an Energy Frontier Research Center funded by the U.S. Department of Energy, Office of Science, Office of Basic Energy Sciences under Award Number DE-SC0001015. Structural analyses were supported by the Robert A. Welch Foundation through a Welch Endowed Chair to H.J.Z. (A-0030). This material is also based upon work supported by the National Science Foundation Graduate Research Fellowship under Grant No. DGE: 1252521. The authors also acknowledge the financial supports of National Science Foundation Small Business Innovation Research (NSF-SBIR) under Grant No. (1632486) and the National Natural Science Foundation of China (Grant Nos. 21571187, 21701187), Taishan Scholar Foundation (ts201511019). S.Y. also acknowledges the Dow Chemical Graduate Fellowship.

Conflict of interest

The authors declare no conflict of interest.

Keywords: heterogeneous catalysis · metal–organic frameworks · pore environments · rare-earth metals

How to cite: *Angew. Chem. Int. Ed.* **2018**, *57*, 5095–5099
Angew. Chem. **2018**, *130*, 5189–5193

[1] a) H. C. Zhou, J. R. Long, O. M. Yaghi, *Chem. Rev.* **2012**, *112*, 673; b) L. J. Murray, M. Dincă, J. R. Long, *Chem. Soc. Rev.* **2009**, *38*, 1294; c) K. Sumida, D. L. Rogow, J. A. Mason, T. M. McDonald, E. D. Bloch, Z. R. Herm, T. H. Bae, J. R. Long, *Chem. Rev.* **2012**, *112*, 724; d) P. Horcajada, R. Gref, T. Baati, P. K. Allan, G. Maurin, P. Couvreur, G. Férey, R. E. Morris, C. Serre, *Chem. Rev.* **2012**, *112*, 1232; e) H. Furukawa, U. Muller, O. M. Yaghi, *Angew. Chem. Int. Ed.* **2015**, *54*, 3417; *Angew. Chem.* **2015**, *127*, 3480; f) Q. C. Xia, Z. J. Li, C. X. Tan, Y. Liu, W. Gong, Y. Cui, *J. Am. Chem. Soc.* **2017**, *139*, 8259; g) S. Sen, N. Hosono, J. J. Zheng, S. Kusaka, R. Matsuda, S. Sakaki, S. Kitagawa, *J. Am. Chem. Soc.* **2017**, *139*, 18313; h) P. Deria, J. E. Mondloch, E. Tylianakis, P. Ghosh, W. Bury, R. Q. Snurr, J. T. Hupp, O. K. Farha, *J. Am. Chem. Soc.* **2013**, *135*, 16801.

[2] H. X. Deng, C. J. Doonan, H. Furukawa, R. B. Ferreira, J. Towne, C. B. Knobler, B. Wang, O. M. Yaghi, *Science* **2010**, *327*, 846.

[3] a) L. J. Liu, K. Konstas, M. R. Hill, S. G. Telfer, *J. Am. Chem. Soc.* **2013**, *135*, 17731; b) L. J. Liu, S. G. Telfer, *J. Am. Chem. Soc.* **2015**, *137*, 3901.

[4] a) S. Yuan, Y. P. Chen, J. S. Qin, W. G. Lu, L. F. Zou, Q. Zhang, X. Wang, X. Sun, H. C. Zhou, *J. Am. Chem. Soc.* **2016**, *138*, 8912; b) S. Yuan, W. G. Lu, Y. P. Chen, Q. Zhang, T. F. Liu, D. W. Feng, X. Wang, J. S. Qin, H. C. Zhou, *J. Am. Chem. Soc.* **2015**, *137*, 3177.

[5] S. Yuan, J. S. Qin, L. F. Zou, Y. P. Chen, X. Wang, Q. Zhang, H. C. Zhou, *J. Am. Chem. Soc.* **2016**, *138*, 6636.

[6] a) D. Alezi, A. M. P. Peedikakkal, L. J. Weselinski, V. Guillerm, Y. Belmabkhout, A. J. Cairns, Z. J. Chen, L. Wojtas, M. Eddaoudi, *J. Am. Chem. Soc.* **2015**, *137*, 5421; b) A. H. Assen, Y. Belmabkhout, K. Adil, P. M. Bhatt, D. X. Xue, H. Jiang, M. Eddaoudi, *Angew. Chem. Int. Ed.* **2015**, *54*, 14353; *Angew. Chem.* **2015**, *127*, 14561; c) Z. J. Chen, L. J. Weselinski, K. Adil, Y. Belmabkhout, A. Shkurenko, H. Jiang, P. M. Bhatt, V. Guillerm, E. Dauzon, D. X. Xue, M. O'Keeffe, M. Eddaoudi, *J. Am. Chem. Soc.* **2017**, *139*, 3265; d) V. Guillerm, L. J. Weselinski, Y. Belmabkhout, A. J. Cairns, V. D'Elia, L. Wojtas, K. Adil, M. Eddaoudi, *Nat. Chem.* **2014**, *6*, 673; e) R. Luebke, Y. Belmabkhout, L. J. Weselinski, A. J. Cairns, M. Alkordi, G. Norton, L. Wojtas, K. Adil, M. Eddaoudi, *Chem. Sci.* **2015**, *6*, 4095; f) D. X. Xue, Y. Belmabkhout, O. Shekhah, H. Jiang, K. Adil, A. J. Cairns, M. Eddaoudi, *J. Am. Chem. Soc.* **2015**, *137*, 5034; g) D. X. Xue, A. J. Cairns, Y. Belmabkhout, L. Wojtas, Y. L. Liu, M. H. Alkordi, M. Eddaoudi, *J. Am. Chem. Soc.* **2013**, *135*, 7660.

[7] a) J. H. Cavka, S. Jakobsen, U. Olsbye, N. Guillou, C. Lamberti, S. Bordiga, K. P. A. Lillerud, *J. Am. Chem. Soc.* **2008**, *130*, 13850; b) M. J. Katz, Z. J. Brown, Y. J. Colón, P. W. Siu, K. A. Scheidt, R. Q. Snurr, J. T. Hupp, O. K. Farha, *Chem. Commun.* **2013**, *49*, 9449; c) G. R. Cai, H. L. Jiang, *Angew. Chem. Int. Ed.* **2017**, *56*, 563; *Angew. Chem.* **2017**, *129*, 578; d) T. C. Wang, N. A. Vermeulen, I. S. Kim, A. B. F. Martinson, J. F. Stoddart, J. T. Hupp, O. K. Farha, *Nat. Protoc.* **2016**, *11*, 149.

[8] a) W. P. Lustig, S. Mukherjee, N. D. Rudd, A. V. Desai, J. Li, S. K. Ghosh, *Chem. Soc. Rev.* **2017**, *46*, 3242; b) J. C. G. Bünzli, C. Piguet, *Chem. Rev.* **2002**, *102*, 1897; c) J. Kido, Y. Okamoto, *Chem. Rev.* **2002**, *102*, 2357; d) T. M. Reineke, M. Eddaoudi, M. Fehr, D. Kelley, O. M. Yaghi, *J. Am. Chem. Soc.* **1999**, *121*, 1651; e) M. D. Allendorf, C. A. Bauer, R. K. Bhakta, R. J. T. Houk, *Chem. Soc. Rev.* **2009**, *38*, 1330; f) Y. J. Cui, Y. F. Yue, G. D. Qian, B. L. Chen, *Chem. Rev.* **2012**, *112*, 1126; g) P. F. Ji, K. Manna, Z. Lin, X. Feng, A. Urban, Y. Song, W. B. Lin, *J. Am. Chem. Soc.* **2017**, *139*, 7004; h) L. Cao, Z. K. Lin, W. J. Shi, Z. Wang, C. K. Zhang, X. F. Hu, C. Wang, W. B. Lin, *J. Am. Chem. Soc.* **2017**, *139*, 7020; i) B. An, J. Z. Zhang, K. Cheng, P. F. Ji, C. Wang, W. B. Lin, *J. Am. Chem. Soc.* **2017**, *139*, 3834.

[9] a) D. W. Feng, Z. Y. Gu, Y. P. Chen, J. Park, Z. W. Wei, Y. J. Sun, M. Bosch, S. Yuan, H. C. Zhou, *J. Am. Chem. Soc.* **2014**, *136*, 17714; b) W. Morris, B. Volosskiy, S. Demir, F. Gandara, P. L. McGrier, H. Furukawa, D. Cascio, J. F. Stoddart, O. M. Yaghi, *Inorg. Chem.* **2012**, *51*, 6443.

[10] a) D. W. Feng, W. C. Chung, Z. W. Wei, Z. Y. Gu, H. L. Jiang, Y. P. Chen, D. J. Darensbourg, H. C. Zhou, *J. Am. Chem. Soc.* **2013**, *135*, 17105; b) J. S. Anderson, A. T. Gallagher, J. A. Mason, T. D. Harris, *J. Am. Chem. Soc.* **2014**, *136*, 16489.

[11] a) D. W. Feng, Z. Y. Gu, J. R. Li, H. L. Jiang, Z. W. Wei, H. C. Zhou, *Angew. Chem. Int. Ed.* **2012**, *51*, 10307; *Angew. Chem.* **2012**, *124*, 10453; b) K. Sasan, Q. P. Lin, C. Y. Mao, P. Y. Feng, *Chem. Commun.* **2014**, *50*, 10390.

[12] a) X. B. Lu, D. J. Darensbourg, *Chem. Soc. Rev.* **2012**, *41*, 1462; b) M. North, R. Pasquale, C. Young, *Green Chem.* **2010**, *12*, 1514; c) W. Y. Gao, Y. Chen, Y. Niu, K. Williams, L. Cash, P. J. Perez, L. Wojtas, J. Cai, Y. S. Chen, S. Q. Ma, *Angew. Chem. Int. Ed.* **2014**, *53*, 2615; *Angew. Chem.* **2014**, *126*, 2653; d) M. H. Beyzavi, R. C. Klet, S. Tussupbayev, J. Borycz, N. A. Vermeulen, C. J. Cramer, J. F. Stoddart, J. T. Hupp, O. K. Farha, *J. Am. Chem. Soc.* **2014**, *136*, 15861.

[13] M. L. Gao, W. J. Wang, L. Liu, Z. B. Han, N. Wei, X. M. Cao, D. Q. Yuan, *Inorg. Chem.* **2017**, *56*, 511.

Manuscript received: March 2, 2018
Accepted manuscript online: March 6, 2018
Version of record online: March 22, 2018

